



1 **Real time rainfall estimation using microwave signals of cellular communication networks:** 2 **a case study of Faisalabad, Pakistan**

3 Muhammad Sohail Afzal¹, Syed Hamid Hussain Shah¹, Muhammad Jehanzeb Masud Cheema¹, Riaz Ahmad²

4 ¹Department of Irrigation & Drainage, Faculty of Agricultural Engineering & Technology, University of Agriculture Faisalabad, Pakistan

5 ²Department of Agronomy, Faculty of Agriculture, University of Agriculture, Faisalabad, Pakistan

6 Correspondence to: Muhammad Sohail Afzal (msohail1227@yahoo.com)

7 **Abstract**

8 Water balance estimate requires high spatio-temporal water balance components and rainfall is
9 one of them. Rainfall is stochastic variable, which varies with respect to space and time. There
10 are different methods for rainfall estimation such as rain gauge, satellite data but the resolution
11 of these methods are very low, which cause over and underestimation of rainfall. A real time
12 rainfall estimation mechanism is tested using commercial cellular networks in Faisalabad, district
13 of Pakistan. The microwave links are used to quantify rainfall intensities and estimate rainfall at
14 high spatio-temporal resolution. The attenuation in electromagnetic signals due to varying
15 rainfall intensities is measured by taking difference between the power transmitted and power
16 received during rainy period and is the measure of the path-averaged rainfall intensity. This
17 rainfall related distortion is converted into rainfall intensity. This technique is applied on a
18 standard microwave communication network used by a cellular communication system,
19 comprising 35 microwave links, and it allow for observation of near-surface rainfall at the
20 temporal resolutions of 15 min. Signal data-set of year 2012-2014 and 2015-2017 is used for
21 calibration and validation respectively with three rain gauge data-set. The accuracy of the
22 method is demonstrated by comparing the daily cumulative rainfall depth of University of
23 Agriculture Faisalabad rain gauge (UAF-RG), Ayub Agriculture Research rain gauge (AR-RG)
24 and Water and Sanitation Authority rain gauge (WASA-RG) with link based rainfall depths
25 estimated from L2, L28 and L34 respectively, reaching r^2 up to 0.97. UAF-RG is considered
26 reference to study the spatial variability of rainfall of all the selected links within the study area,
27 observed 10%-60% average spatial error of all links with the reference UAF-RG. All the results
28 show that microwave links are potentially useful compared to the low resolution methods of
29 rainfall estimation and can be used for effective water resources management.

30 **Keywords:** Rainfall, microwave signal data, Interpolation, rain gauge data and path average
31 rainfall intensity



Nomenclature

PL	Path length (distance between two towers)
D-(UAF-RG)	Distance of link from University of Agriculture Rain Gauge
CV	Coefficient of variance
r^2	Coefficient of determination
IDW	Inverse Distance Weighted
TRMM	Tropical Rainfall Measuring Mission
GPM	Global Precipitation Measurement
PMD	Pakistan Meteorological Department
D-(AR-RG)	Distance of link from Ayub Research Rain Gauge
D-(WASA-RG)	Distance from Water and Sanitation Authority Rain Gauge

32

33 1. Introduction

34 The management of water resources requires high temporal and spatial information of
35 rainfall. Rainfall is considered as an important input parameter for hydrological model that's
36 why it needs to be managed and measured very carefully on high spatial and temporal basis. Any
37 small error of a large water balance component that is rainfall can produce significant error in the
38 small components such as runoff, leaching, capillary up flow from shallow groundwater.
39 Without exact measurement of rainfall, agricultural crops, surface and groundwater resources
40 cannot be managed on sustainable basis (Yilmaz et al., 2005; Berndtsson and Niemczynowicz
41 1988).

42 Aerial rainfall for catchment and basin is normally interpolated from rain gauge, radar and
43 satellite data but these sources provide very low resolution data and all these instruments has
44 their own challenges. The spatial interpolation of point measurements in heterogeneous
45 landscapes and mountains result in erroneous estimates. Dense networks are needed that are
46 difficult to establish and maintain in under developing countries. Rainfall estimation by using
47 satellite data cannot provide full coverage of rainfall due to low spatio-temporal resolution.
48 There are geostationary satellite observations are available having temporal resolution of 15 min
49 but are often very indirect e.g. estimates through cloud physical properties (Roebeling and
50 Holleman 2009). There is another new product of NASA called GPM mission having spatial



51 resolution 0.1° and temporal resolution of 30 min but this is still very low resolution as compared
52 to the rainfall estimated by microwaves links (Hou et al., 2014; Rios Gaona et al., 2016).
53 Similarly another data source which is mostly used is TRMM having spatial resolution 0.25° and
54 temporal resolution minimum 3 hours .The downscaling of satellite image is a technique that can
55 estimate rainfall for a smaller range of distance, but this technique is indirect technique and
56 produces biasness and uncertainty in results. The rainfall estimated from radar normally
57 deteriorates for longer ranges from radar.

58 In Pakistan rain gauge networks are managed and operated by Pakistan Meteorological
59 Department (PMD). There are total 97 rain gauge stations in Pakistan which include 28 in
60 Punjab, 19 in KPK, 05 in Azad Kashmir, 09 in Northern Areas, 27 in Sindh-Balochistan and 09
61 observatories controlled by Geophysics Quetta which are insufficient to capture high spatio-
62 temporal rainfall (PMD Website). The intensity of telecommunication tower is greater than the
63 magnitude of rain gauges. Therefore the main focus of the study is to quantify the rainfall due to
64 the signal attenuation and promote the use of microwave links for rainfall estimation in Pakistan.

65 The basic concept behind the rainfall estimation from signal attenuation is that the signal
66 that travels between the two towers attenuates due to rainfall intensity and this attenuation
67 depends upon the rainfall duration and rainfall intensity, as more intensity of rainfall will create
68 more signal distortion. As the number of raindrops and intensity of rainfall increases, the
69 attenuation of link also increases, which subsequently reduced the received power at the other
70 end of the link. The power received at the other end of the link is considering a byproduct of the
71 communication between the networks (Zinevich et al., 2008; Goldshtein et al., 2009; Zinevich et
72 al., 2009; Overeem et al.,(2011,2013,2016);Messer et al., 2006; Leijnse et al., 2007b; Zinevich et
73 al., 2009; van het Schip et al. 2017, Rios Gaona et al., 2015). This new advancement of using
74 link data for rainfall estimation is very helpful to estimate the rainfall at a very high resolution
75 which will further use for flood prediction, drought management, crop productivity and risky
76 climate warning. Similarly massive deployment of these microwave links provides a
77 complementary network to measure rainfall, especially in countries where rain gauges are scarce
78 or poorly maintained, and where ground-based weather radars are not (yet) deployed
79 (Doumounia et al., 2014).

80 In section 2, the detail of cellular communication link and rain gauge data information is
81 explained. In section 3, description about how to use signal data to measure path-averaged

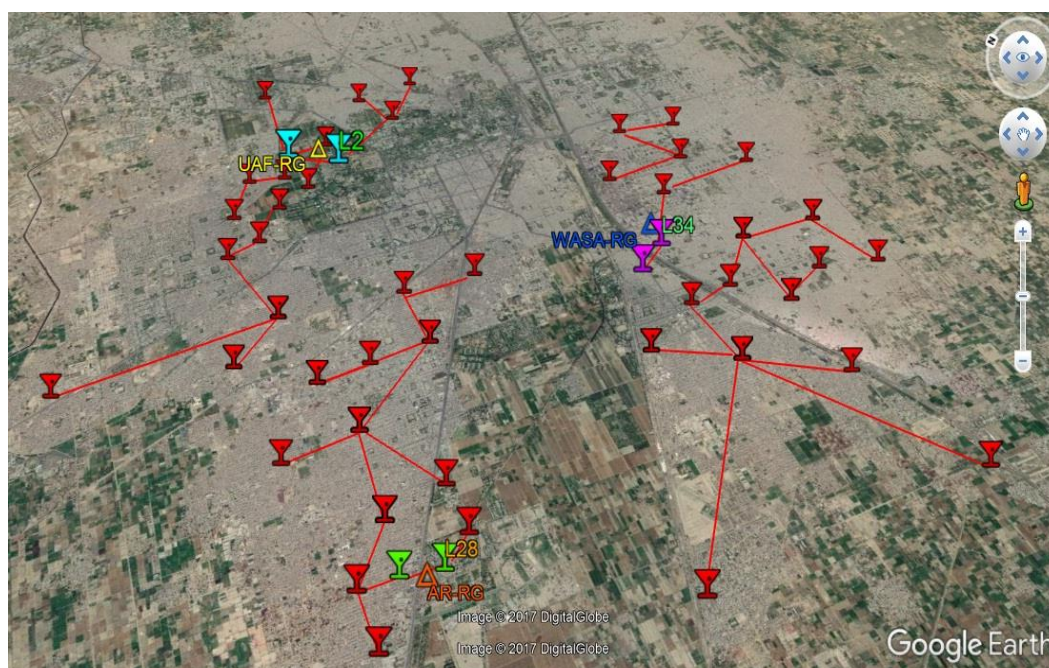


82 rainfall intensity, mapping technique for rainfall map and other methodology to study the spatial
83 variability of rainfall and in section 4, final discussion and conclusion is elaborated.

84 2. Type of data used

85 2.1. Microwave link data

86 In order to estimate the path-averaged rainfall intensities, signal data of 35 selected links in
87 Faisalabad is obtained from international telecommunication Network Company Telenor,
88 working in Pakistan. The maximum and minimum received power over 15 min temporal
89 resolution having 38 GHz frequency is used. Figure 1 explains the location of 35 selected
90 microwave links and location of rain gauges. It is clear from the Fig.1 that L2, L28 and L34 are
91 close to UAR-RG, AR-RG and WASA-RG respectively. All the selected links are vertically
92 polarized and in the radius of 225 km² area. The data format required to process the code is
93 acquired from Overeem et al. (2016). Total 32 and 33 days from years 2012-2014 and 2015-2017
94 are selected for calibration and validation of link based approach with standard rain gauges data-
95 set respectively. The path length, i.e. distance between the sender and receiver, for all the
96 selected links is between 0.50-2.5 km.



97



98 **Figure 1.** Map of study area with location of selected microwave links (red, zinc, green and
99 purple towers), and triangles: yellow color (University of Agriculture), orange color (Ayub
100 Research) and blue color (Water and Sanitation Authority) rain gauge.

101 2.2. Rain gauge data

102 The employed rain gauges data are obtained from three different rain gauge stations namely
103 UAF-RG, WASA-RG and AR-RG, operated by University of Agriculture Faisalabad, Ayub
104 Agriculture research and Water and Sanitation Authority Faisalabad respectively. The data
105 provided by all these rain gauge stations are daily cumulative rainfall values against each rainy
106 day. For calibration and validation purpose, signal based rainfall having 15 min resolution data is
107 converted into daily cumulative rainfall value for each day to compare it with UAF-RG, WASA-
108 RG and AR-RG stations. Independent calibration and validation of three selected links i.e. L2,
109 L28 and L34 against UAF-RG, AR-RG and WASA-RG respectively are performed and by
110 considering UAF-RG as a reference point, calibration and validation of all the selected links
111 against UAF-RG are performed to study the spatial variability of rainfall

112 3. Methodology

113 3.1. Rainfall retrieval for signal based rainfall

114 Microwave links are the main source of communication between the telecommunication
115 towers and these microwave links attenuate due to rainfall intensity (Upton et al., 2005). This
116 distortion in the signal can be measured by using power law studied by Atlas and Ulbrich (1977)
117 which is the relationship between rainfall and specific attenuation

$$118 \quad r = cz^b \quad (1)$$

119 In Eq. (1) z is the specific attenuation, r is the intensity of rainfall (mmh^{-1}), c is the
120 coefficient and b is the exponent and the values of these coefficient and exponent depend upon
121 polarization, frequency of the signal, temp of the surrounding, water phase and other important
122 factor which include drop size distribution, canting angle distribution and shape of the rain drop
123 (Jameson, 1991; Berne and Uijlenhoet, 2007; Leijnse et al., 2010a) and further explained by
124 Overeem et al., (2016). During rainy period the entire length (km) of the signal between the two
125 tower attenuate (dB) and thus the intensity of the rainfall is given by



$$126 \quad F_{\text{ref}}(L) - F(L) = A_m = \int_0^L z(d) ds = \int_0^L \left[\frac{r(d)}{c} \right]^{1/b} ds \quad (2)$$

127 In Eq. (2) F_{ref} is the reference signal level, d stands for the entire length of the signal and F
128 (L) is the received power (dBm). After approximation final form of power law is given below
129 (Overeem et al., 2011, 2013, 2016)

$$130 \quad \langle r \rangle = c \left[\frac{F_{\text{ref}}(L) - F(L)}{d} \right]^b \quad (3)$$

131 The value of coefficient c and exponent b as explained by Overeem et al., (2016). Berne and
132 Uijlenhoet (2007) studied that how link length, frequency, precise drop size division effect the
133 average rainfall intensity for links having frequency range between 12 to 38 GHz. They
134 concluded that the value of coefficient c and exponent b will depend on the frequency of the link
135 and not account much on the length of the signal. If the length of the signal increases, the
136 frequency of the microwave link decreases. The reason behind is that if length increases, than the
137 effect of rain drop on the frequency does not gives the best result, therefore links are usually
138 selected within acceptable distances for making sure strong signal strength.

139 The concept of rainfall estimation is derived from the minimum and maximum received
140 power having 15 min high resolution. This maximum and minimum received power is converted
141 into corrected minimum and corrected maximum received power by comparing with reference
142 signal power. In the first step, the pre-processing of link data is done using the code developed in
143 R software (Overeem et al., 2016). In this step, the signal data of previous day and present day is
144 converted into one file based on the selection of links having frequency of 12-42 GHz. If a
145 unique link contains more than one record, that link is removed during the pre-processing,
146 because one unique link can have only one record for a specific time interval. Also in this step, it
147 is confirmed that whether frequency, link coordinates, and path length of a unique link remains
148 same in whole day. This criteria is very important because these parameters should not change
149 during a day, if this is the case, that link is also removed.

150 Based on above checks, one file is prepared which is free from errors. In the next step, the
151 file prepared in the first step is used for further processing related with categorization of wet and
152 dry signals using the code in R developed separately for this step (Overeem et al., 2016). In the
153 next step, the link having both ends within 15 km from either side end selected link. Based on the



154 threshold value of signal, the wet and dry signals are identified (Overeem et al., 2011, 2016). In
155 the third step rainfall intensities are estimation based on the corrected maximum and minimum
156 received signal power of the file prepared in the above step using the power law relationship
157 (Overeem et al., 2011,2016), Leijnse et al., 2007, van het Schip et al. 2017, Rios Gaona et al.,
158 2015).

159 There are many type of errors that may come in the way to estimate the rainfall intensity and
160 these errors may be because of the reflection and refraction of the beam, dew formation on the
161 surface of the antennas, antenna icing, scintillation, multipath, reliable absorption by the
162 atmosphere constituents (Upton et al., 2005). According to Upton et al. [2005] there is a very
163 small fluctuation in the received signal power during dry season as compared to the fluctuation
164 in the received power when there is no rain. There is another source of error in rainfall estimation
165 because of the water films on the tower antenna .This type of signal attenuation is a major
166 source of error which is modified by (Kharadly and Ross 2001; Minda and Nakamura 2005;
167 Leijnse et al., 2007a, 2007b, 2008). When there is large distance between the link the change due
168 to wet antenna is very small because the signal attenuation due to rainfall is very small (Leijnse
169 et al., 2008).

170 The temporal sampling describes the number of sample per unit time and used this for
171 collection of the samples. Leijnse et al. (2008) explained the three type of sampling strategies,
172 which is averaged, intermittent and continuous. The intermittent and averaged strategies are
173 mostly used for cellular communication link monitoring. In these two types of sampling
174 strategies, signal power is observed over averaged 15 min resolution or sample may be selected
175 in the middle of 15 min period. The intermittent sampling strategies has been used in the
176 research for rainfall estimation, which is similar to the Messer et al. (2006) which is the
177 maximum and minimum received power, F_{\min} and F_{\max} are collected over 15 min resolution.
178 There is another error that may occur and is responsible for the decrease the availability of data
179 is due to the heavy rainfall. This type of error may be due to the storage issue arrives in the
180 server of the telecommunication company. Overeem et al. (2016) suggested some fixed
181 parameters on the basis of these errors and all these recommend parameters values are used in
182 the paper.

183



184 3.2. Verification methodology

185 For calibration and validation purpose path-averaged rainfall intensities estimated from the
186 signal data having 15 min resolution are converted in to daily (24hrs) cumulative rainfall value
187 against each day to compare it with daily (24hrs) cumulative rainfall values of UAF-RG, AR-RG
188 and WASA-RG. Independent calibration and validation of L2, L24 and L34 are performed
189 against UAF-RG, AR-RG and WASA-RG respectively.

190 3.3. Percentage error analysis

191 By considering UAR-RG as reference point to study the spatial variability of rainfall in the
192 study area, calibration and validation is performed for all 35 no of selected links between UAF-
193 RG and signal based rainfall depths. After estimated signal based rainfall, percentage error for all
194 the all selected links is calculated according to the Eq. (4) and Eq. (5), where d is cumulative
195 signal based rainfall, f is cumulative UAF-RG rainfall depth, PD is percentage error of each day
196 and L no is link number.

197 Percentage error analysis for each selected link against each day (PD) = $\left(1 - \left(\frac{d}{f}\right)\right) * 100$ (4)

198 Average percentage spatial error for all selected days for each link = $\frac{\sum_{i=1}^n PD_i}{L\ no}$ (5)

199 3.4. Rainfall mapping

200 Path-averaged rainfall estimated from cellular microwave links are spatially interpolated
201 to obtain the rainfall maps. Overeem et al., (2016, 2015, 2013); Rios Gaona et al., (2015)
202 suggested two type of interpolation techniques i.e. ordinary kriging (OK) and inverse distance
203 weighted (IDW). Both these interpolation methods are well suited for dealing with spatially
204 disturbed data locations. The ordinary kriging requires variogram model, so it is not possible to
205 reboust such variogram in this study because of limited data-set. IDW technique is used to
206 interpolate the rainfall maps of study area. The path-averaged rainfall estimated from link
207 approach is considered at the center of the sender and receiver, so that point data can be used in
208 IDW interpolation. Rainfall maps are prepared in GIS by using IDW interpolation technique to
209 study spatial variation in rainfall estimates between signal and rain gauge rainfall depths.

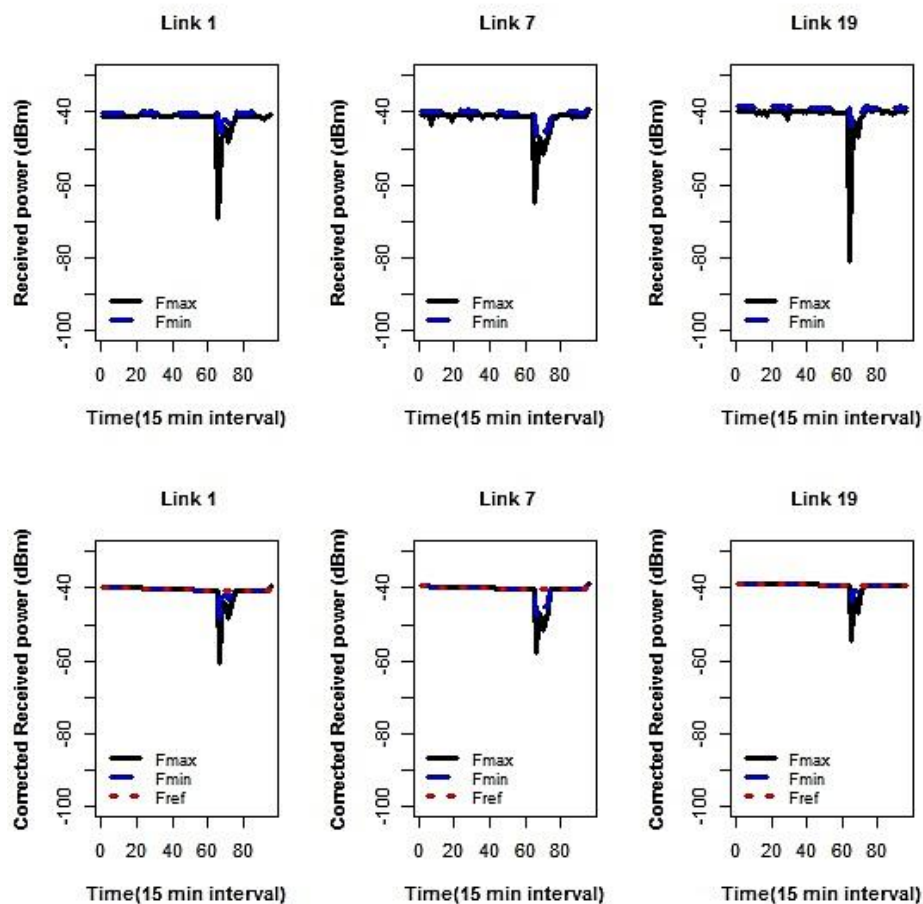
210



211 **4. Result and Discussion**

212 **4.1. Maximum, minimum received, corrected maximum and minimum received power**

213 The signal attenuation due to rainfall is the main factor to find the rainfall intensities which
214 is the difference between the received signal level and some reference signal level which is
215 representation of the dry period when there is no rain. The attenuation in the signal is estimated
216 by using the procedure explained in the section 3 and compared that attenuation with the
217 reference signal power to find corrected maximum power received and corrected minimum
218 power received (Overeem et al., 2015, 2016). Overeem et al., (2016), van het Schip et al. (2017),
219 Rios Gaona et al., (2015) presented graphs showing the minimum and corrected minimum
220 received power compared with gauge-adjusted radar having 15 min resolution but due to no data
221 availability of radar with same 15 min temporal resolution, it is not possible to make such
222 comparison in this study so only attenuation due to rainfall intensity is shown in fig.2. The Fig. 2
223 shows the maximum and minimum power received and corrected minimum and maximum
224 power received compared with reference signal level. The top (right, middle and left) plots
225 present attenuation due to rainfall of three different links and bottom (right, middle and right)
226 plots present corrected maximum and minimum received power which is compared with
227 reference signal level. It is clear from Fig 02 that all the links show the different attenuation due
228 to rainfall intensity but the time of distortion remains the same in all the links, which is located
229 index number 66 to 70 time interval.



230

231 **Figure 2.** Top (right, middle and right) plots present maximum received power (black line) and
232 minimum received power (blue line) for three different links for 12 May 2014. Bottom (right,
233 middle and left) plots present maximum corrected received power (black line) and minimum
234 corrected received power (blue line) and reference signal level (red line) for three different links
235 for same day dated 12 May 2014. There are total 96 time intervals having 15 min resolution in
236 each plot against each day (24 hours).

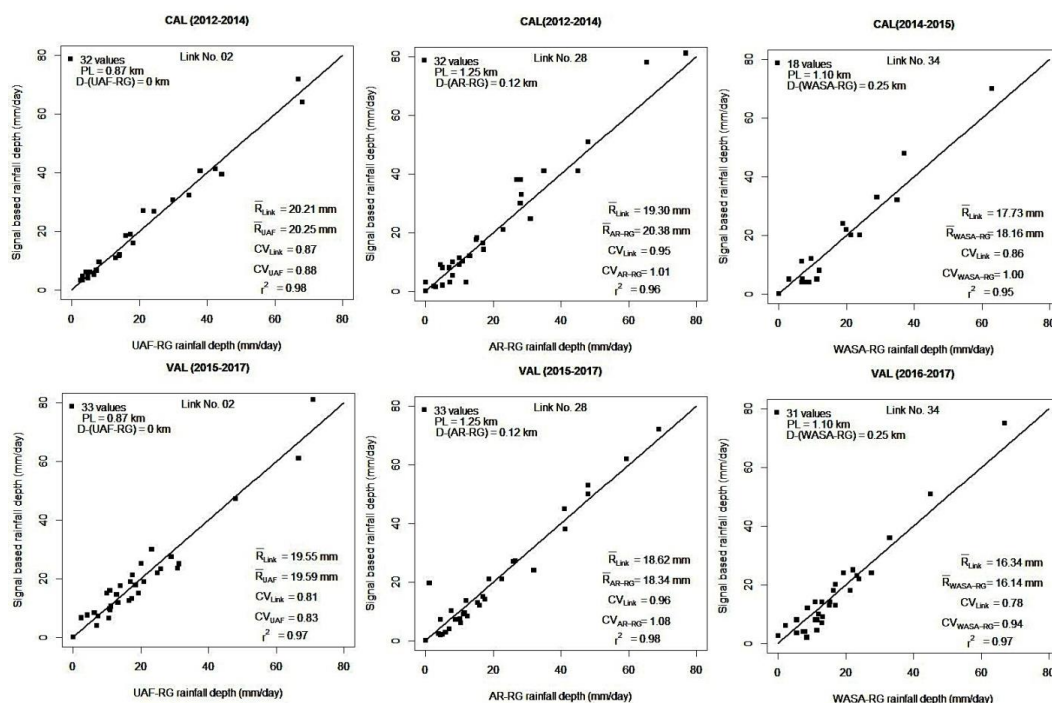
237

238



239 **4.2. Calibration and validation of signal based rainfall with standard rain gauge data**
240 **operated in Faisalabad.**

241 The rainfall estimated from link based approach having 15 min resolution is converted
242 into daily cumulative rainfall depth to compare it with the daily cumulative rainfall depth of rain
243 gauge operated by different institutions in Faisalabad. The comparisons are observed for three
244 different cases of spatiotemporal aggregation, for the daily commutative rainfall depths of UAF-
245 RG, AR-RG and WASA-RG with link based rainfall depths estimated from L2, L28 and L34
246 respectively. This study tests the performance of the 32 days for calibration and 33 from
247 validation from years 2012-2014 and 2015-2107 respectively. Figure. 3 Top (right, middle and
248 left) plots and bottom (right, middle and left) plots present calibration and validation of links
249 with standard rain gauges. All the scatter plots in fig.3 summarizes the values of the mean
250 rainfall depth (R_{Link} , R_{UAF-RG} , R_{AR-RG} and $R_{WASA-RG}$), the coefficient of variation (of the residuals)
251 CV, and the coefficient of determination r^2 (i.e. the squared correlation coefficient) for the three
252 cases of spatiotemporal aggregation, for link based and standard rain gauges rainfall depths. It is
253 clear from fig. 3 that coefficient of determination for L2, L28 and L34 compared with UAF-RG,
254 AR-RG and WASA-RG are 0.98, 0.96 and 0.95 respectively for calibration data-set, whereas
255 coefficient of determination for L2, L28 and L34 compared with UAF-RG, AR-RG and WASA-
256 RG are 0.97, 0.98 and 0.97 respectively for validation data-set.



257

258 **Figure 3.** Calibration and validation of signal based rainfall with standard rain gauges operated
 259 in Faisalabad. Left (top and bottom) plots present calibration and validation of L2 with UAF-
 260 RG, middle (top and bottom) plots present calibration and validation of L28 with AR-RG and
 261 right(top and bottom) plots present calibration and validation of L34 with WASA-RG.

262 **4.3. Calibration and validation of signal based rainfall for the all selected links with UAF-
 263 RG to study the spatial variability of rainfall.**

264 **4.3.1. Calibration and validation**

265 The UAF-RG is used as a reference point to study the spatial variability of rainfall in the
 266 selected study area. The cumulative rainfall depths of UAF-RG are compared with all the
 267 selected 35 links based rainfall depth to study the spatially variability within area of 225 km².
 268 Overeem et al. (2011, 2013, and 2016), Van het Schip et al (2017), Rios Gaona et al., (2015)
 269 used a gauge-adjusted radar data set to calibrate and validate the microwave link rainfall retrieval
 270 algorithm but in this study due to limited data availability of radar, daily cumulative rainfall
 271 values of UAF-RG are compared with the daily cumulative rainfall depth measured by link based

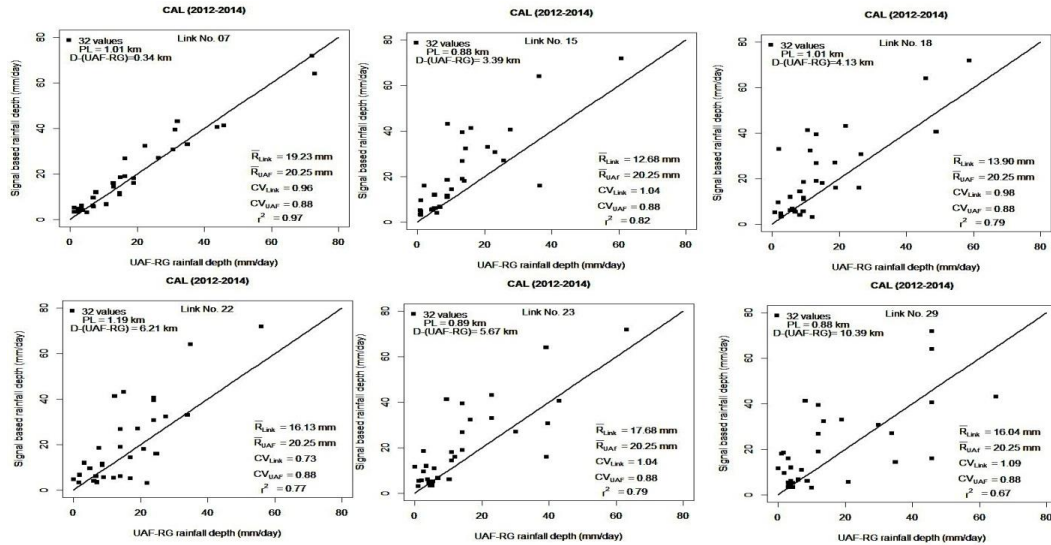


272 approach for all the selected links. For calibration purpose, total 32 numbers of days are selected
273 for years 2012-2014. The distance of all the selected links from the reference UAF-RG and
274 distance between the transmitter and receiver of all the links are measured. The links 02 was very
275 close to reference UAF-RG nearly 0 km distance and all the other remaining points are in the
276 area of 225 km² around the UAF-RG.

277 The comparisons are carried out on the basis of scatter density plots and three metrics:
278 mean rainfall, coefficient of variation (CV), and coefficient of determination (r^2). Figure 04
279 explains scatter density plots between the daily commutative signal based and daily cumulative
280 rainfall of UAF-RG station rainfall depth (mm/day). The statistical analysis between observed
281 UAF-RG and signal based rainfall is analyzed. The values of CV, r^2 , and the average
282 commutative rainfall measured using UAF-RG, as indicated by R_{UAF} and average commutative
283 rainfall depth using signal approach, indicated by R_{LINK} , are included in the plots. The coefficient
284 of variation CV and coefficient of determination for link which is close to the UAF-RG show
285 significant results, but as the distance of links increases from the reference UAF-RG, level of
286 significance decreases. It is clear from the fig.3 that for L7, L15, L18, L22, L23 and L29, as the
287 distance increases 0.34 km, 3.39 km, 4.13km, 6.21 km, 5.67 km and 10.39 km respectively from
288 Reference UAF-RG, level of significance i.e. coefficient of determination decreases. For
289 calibration data-set, the coefficient of determination for L7, L15, L18, L23, L22 and L29, are
290 0.97, 0.82, 0.79, 0.91, 0.79 and 0.67 respectively, Similarly data-set having frequency 38 GHz is
291 used in this study for the validation purpose. The same links are used for the validation purpose
292 as used from calibration purpose but data-set used are of different time period. For validation
293 purpose data-set of years 2015-2017 are used and total 33 rainy included non rainy days are
294 selected. Figure 05 explains validation scatter density plots between the daily cumulative signal
295 based and daily cumulative rainfall of UAF-RG station. The statistical analysis between
296 observed UAF-RG and signal based rainfall is analyzed. It is clear from the fig.4 that for L7,
297 L15, L18, L23, L22 and L29, as the distance increases 0.34, 3.39, 4.13, 6.21, 5.67 and 10.39
298 respectively from Reference UAF-RG, level of significance decreases. For validation data-set,
299 the coefficient of determination for L7, L15, L18, L23, L22 and L29, are 0.96, 0.79, 0.82, 0.78,
300 0.71 and 0.67 respectively. All the above results proved that rainfall is stochastic and erratic
301 pattern variable, as the distance increases from reference UAF-RG due to spatial variation,
302 rainfall depth increases or decreases. Similarly for all selected 35 links, as the distance increases

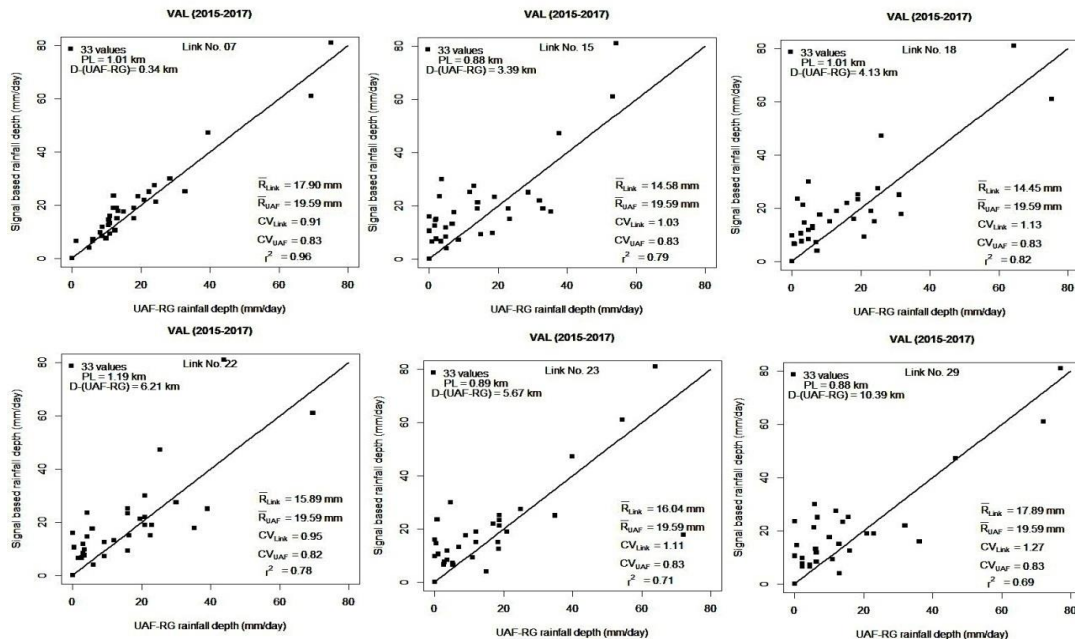


303 from the reference point UAF-RG, the spatial variability fluctuates due to spatial variation in
 304 rainfall intensity.



305

306 **Figure 4.** Scatter density plots of calibration data-set of daily (24hr) cumulative rainfall depths
 307 of signal data of 33 no of days against daily cumulative rainfall depths of UAF rain gauge.



308

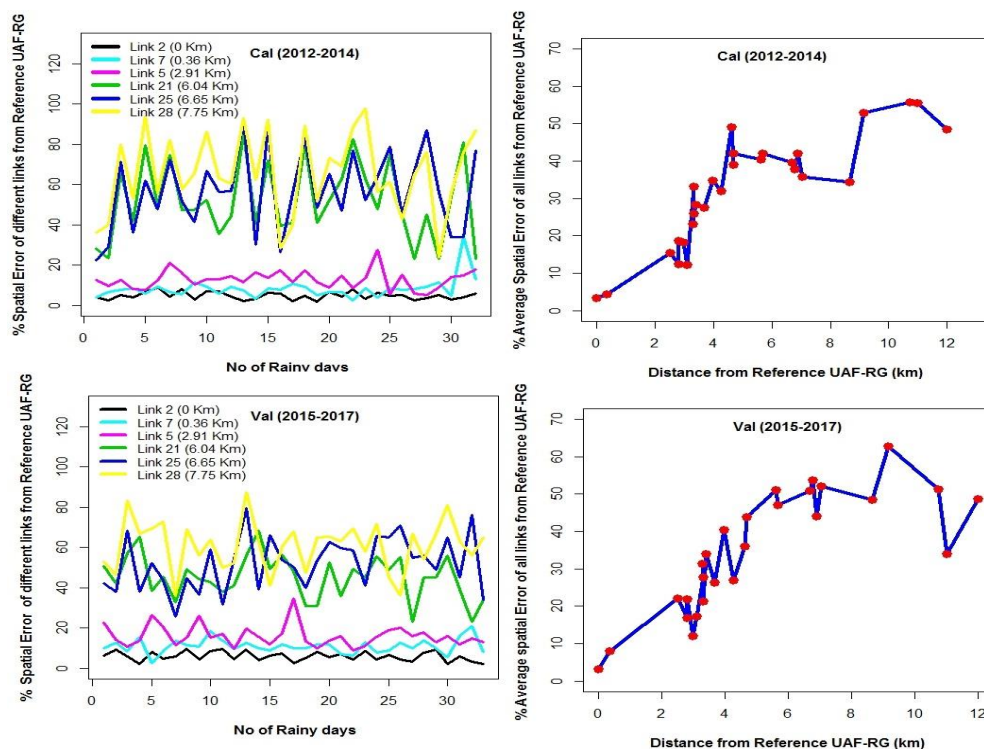


309 **Figure 5.** Scatter density plots of validation data-set of daily (24hr) cumulative rainfall depths
310 of signal data of 33 no of days against daily cumulative rainfall depths of UAF rain gauge.

311 **4.3.2. Spatial percentage error analysis**

312 As it is discussed that there are mostly two sources available for rainfall estimation in
313 Pakistan, which is rain gauge and satellite data. There are limited number of rain gauge networks
314 operating in Indus basin irrigation system (IBIS), which is the largest irrigation system in the
315 world, similarly rainfall estimated by satellite is also of low spatio-temporal resolution, so it is
316 declared as data limited basin (Cheema 2012). Even the instruments which are installed on the
317 existing meteorological stations in Pakistan are outdated and of low spatio-temporal resolution,
318 so these low resolution data is used to estimated rainfall in basins and catchments, which is not
319 the true presentation of the reality because rainfall is stochastic variable and its varies within
320 radius of 1-2 km. Because of the factors discussed above, it is needs of the time that system
321 should be established that provide high spatio-temporal resolution data, which is used for water
322 resources management. Keeping in view of all these factors, rainfall is estimated by using signal
323 based approach and by considering UAF-RG as reference point, percentage spatial error analysis
324 is performed in the study area.

325 Figure 06 left (top and bottom) plots present percentage spatial variation of different
326 links against no of rainy days from reference point UAR-RG. For calibration and validation data-
327 set, the percentage spatial error for links no L2, L5, L7, L21, L25, and L28 varies between 20%-
328 80% for different no of rainy days. It is clear from Fig. 06 left (top and bottom) plots that the
329 percentage Error associated with spatial variation of rainfall from reference point (UAF-RG) i.e.
330 the L2, L5 and L7 are close to reference UAF-RG, so there is small spatial error exist between
331 these links, but the L21, L25 and L28 are far away from the UAF-RG reference point, so there is
332 more spatial error exist. It is clear as the distance increase from the reference point point (UAF-
333 RG) percentage error varies due to spatial variation of rainfall. Similarly fig.6 right (top and
334 bottom) plots presents overall average percentage spatial error of all the selected links against the
335 distance from reference UAF-RG. It is clear from the fig.6 right (top and bottom) plots that as
336 the distance from the reference UAF-RG increases, for calibration and validation data-set,
337 overall percentage average spatial error of all the selected links from reference UAF-RG varies
338 between 10%-50% and 10%-60% respectively, which is logical and makes sense.

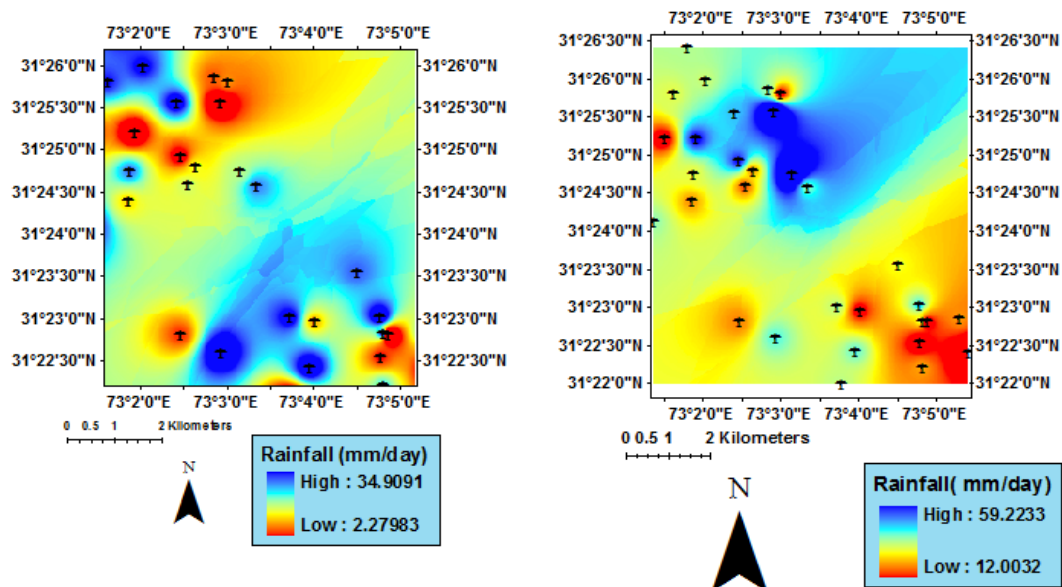


339

340 **Figure 6.** Left (top and bottom) plots present calibration and validation of percentage spatial
 341 error analysis of different links against no of rainy days. Right (top and bottom) plots present
 342 calibration and validation of percentage average spatial error of all links from reference UAF-
 343 RG.

344 4.3.3. Rainfall mapping

345 The rainfall maps are prepared in GIS by using IDW technique for rainfall event of 10
 346 March 2014 and 23 July 2016. Figure 07 explains how rainfall varies within area of 225 Km².
 347 The rainfall varies between 2 to 34 mm and 12 to 59 mm for 10 March 2014 and 23 July 2016
 348 respectively and whereas rainfall recorded by UAF-RG on 10 March 2014 and 23 July May 2016
 349 is 19mm and 40mm respectively and similarly rainfall recorded by WASA-RG on 10 March
 350 2014 and 23 July May 2016 is 30mm and 26.3mm respectively. So one point based value is not a
 351 presentation of whole study area because rainfall varies even within a distance of 1-2 km.



352

353 **Figure 7.** Signal based daily cumulative rainfall depths for all links on 10 March 2014 (left
354 panel). Signal based cumulative rainfall depths for all links on 23 July 2016 (right plot). (Black
355 tower represent different links location)

356 5. Conclusion and recommendation

357 The output of this paper shows that estimation of high resolution rainfall from the signal
358 data of cellular communication network is the first step towards developing local climatic zones,
359 which can contribute significantly in determining the components of water balance. The
360 measurement of rainfall from the signal data of cellular communication network is a novel
361 approach to obtain very high spatio-temporal resolution rainfall. The reason is that other
362 resources such as satellite and rain gauges data cannot provide rainfall data for such a high 15
363 min resolution. There are total 97 rain gauges installed by PMD which are insufficient to capture
364 high spatial and temporal resolution rainfall. Similarly satellite data which include data from
365 TRMM having spatial resolution 0.25° and minimum 3 hour temporal resolution, similarly GPM
366 which is recently introduced having spatial resolution 0.1° and 30 min temporal is not sufficient to
367 presents the real situation. Therefore rainfall estimation by using signal processing is the needs



368 of hour and best suited in under developing country like Pakistan because readily existing setup
369 is used and there is no need of any extra cost of infrastructure or any setup required.

370 Commercial microwave links data of six years are used for rainfall estimation which
371 includes years 2012- 2014 for calibration and 2015-2017 for validation with UAF-RG, AR-RG
372 and WASA-RG respectively. This study proved that using microwave links for rainfall
373 estimation is very beneficial especially for both rural and urban areas. The algorithm developed
374 is highly low-cost and is a first step for the rainfall estimation from the signal data over the entire
375 area of Pakistan. The spatial error analysis also proved that rainfall is a stochastic variable. This
376 new technology has a great potential for calibration and validation for weather radar, assimilation
377 of different type of weather predication model or ground trusting of rainfall measured by using
378 satellite images.

379 This novel approach of measuring rainfall using the cellular communication network is the
380 Information and Communication Technology (ICT) revolution, which will definitely enhance the
381 role of ICT in agriculture and surface and groundwater resources on sustainable basis.

382 **Acknowledgements**

383 The authors would like to thanks Telenor Pakistan for providing the signal data and Dr Aart
384 Overeem, Dr Lenijine Hidde, Research Officers in KNMI Netherlands for providing the
385 technical support for processing of signal data. We are thankful to funding agency USAID

386 **References**

- 387 Atlas, D. and C. W. Ulbrich.: Path- and area-integrated rainfall measurement by microwave
388 attenuation in the 1–3 cm band, *J. Appl. Meteorol.*, 16, 1322–1331, 1977.
- 389 Berndtsson, R., and J. Niemczynowicz.: Spatial and temporal scales in rainfall analysis—Some
390 aspects and future perspectives, *J. Hydrol.*, 100, 293–313, 1988.
- 391 Berne, A., and R. Uijlenhoet.: Path-averaged rainfall estimation using microwave links:
392 Uncertainty due to spatial rainfall variability, *Geophys. Res. Lett.*, 34, L07403, doi:
393 10.1029/2007GL029409, 2007.
- 394 Cheema, M.J.M.: Understanding water resources conditions in data scarce river basins using
395 intelligent pixel information, Case: Tran’s boundary Indus Basin. TU Delft, Delft University of
396 Technology, 2012.



- 397 Doumounia, A., Gosset, M., Cazenave, F., Kacou, M., and Zougmore, F.: Rainfall monitoring
398 based on microwave links from cellular telecommunication networks: first results from a West
399 African test bed, *Geophys. Res. Lett.*, 41, 6016–6022, doi:10.1002/2014GL060724, 2014.
- 400 Goldshtein, O., H. Messer, and A. Zinevich.: Rain rate estimation using measurements from
401 commercial telecommunications links, *IEEE Trans. Signal Process.*, 57, 1616–1625,
402 doi:10.1109/TSP.2009.2012554, 2009.
- 403 Rios Gaona, M. F., Overeem, A., Leijnse, H., and Uijlenhoet, R.: First-year evaluation of GPM-
404 rainfall over the Netherlands: IMERG Day-1 Final Run, *J. Hydrometeorol.*, in review, 2016.
- 405 Jameson, A., A comparison of microwave techniques for measuring rainfall, *J. Appl. Meteorol.*,
406 30, 32–54, 1991.
- 407 Kharadly, M. M. Z., and R. Ross.: Effect of wet antenna attenuation on propagation data
408 statistics, *IEEE Trans. Antennas Propag.*, 49, 1183–1191, 2001.
- 409 Leijnse, H., R. Uijlenhoet, and J. N. M. Stricker.: Hydrometeorological application of a
410 microwave link: 2. Precipitation, *Water Resour. Res.*, 43, W04417,
411 doi:10.1029/2006WR004989, (2007a).
- 412 Leijnse, H., R. Uijlenhoet, and J. N. M. Stricker.: Rainfall measurement using radio links from
413 cellular communication networks, *Water Resour. Res.*, 43, W03201,
414 doi:10.1029/2006WR005631, (2007b).
- 415 Leijnse, H., R. Uijlenhoet, and J. N. M. Stricker.: Microwave link rainfall estimation: Effects of
416 link length and frequency, temporal sampling, power resolution, and wet antenna attenuation,
417 *Adv. Water Resour.*, 31, 1481–1493, doi:10.1016/j.advwatres.2008.03.004, 2008.
- 418 Leijnse, H., R. Uijlenhoet, and A. Berne.: Errors and uncertainties in microwave link rainfall
419 estimation explored using drop size measurements and high-resolution radar data, *J.*
420 *Hydrometeorol.*, 11, 1330–1344, doi:10.1175/2010JHM1243.1, (2010a).
- 421 Leijnse, H and R. Uijlenhoet.: Precipitation measurement at CESAR, the Netherlands, *J.*
422 *Hydrometeorol.*, 11, 1322–1329, doi:10.1175/2010JHM1245.1, (2010b).
- 423 Messer, H. A., A. Zinevich, and P. Alpert.: Environmental monitoring by wireless
424 communication networks, *Science*, 312, 713, 2006.
- 425 Hou, A. Y., Kakar, R. K., Neeck, S., Azarbarzin, A. A., Kummerow, C. D., Kojima, M., Oki,
426 R., Nakamura, K., and Iguchi, T.: The global precipitation measurement mission, *B. Am.*
427 *Meteorol. Soc.*, 95, 701–722, doi:10.1175/BAMS-D-13-00164.1, 2014.



- 428 Minda, H., and K. Nakamura.: High temporal resolution path-average rain gauge with 50-GHz
429 band microwave, *J. Atmos. Oceanic Technol.*, 22, 165–179, 2005.
- 430 Overeem, A., H. Leijnse, and R. Uijlenhoet.: Quantitative precipitation estimation using
431 commercial microwave links, *IAHS Red Book Symp. Proc.*, accepted, 2011.
- 432 Overeem, A., H. Leijnse, and R. Uijlenhoet.: Retrieval algorithm for rainfall mapping from
433 microwave links in a cellular communication network. *Atmos. Meas. Tech.*, 9, 2425–2444, 2016,
434 doi:10.5194/amt-9-2425-2016, 2016.
- 435 Roebeling, R. A. and Holleman, I.: SEVIRI rainfall retrieval and validation using weather radar
436 observations, *J. Geophys. Res.*, 114, D21202, doi:10.1029/2009JD012102, 2009.
- 437 Schleiss, M., and A. Berne.: Identification of dry and rainy periods using telecommunication
438 microwave links, *IEEE Geosci. Remote Sensing Lett.*, 7, 611–615,
439 doi:10.1109/LGRS.2010.2043052, 2010.
- 440 Upton, G. J. G., A. R. Holt, R. J. Cummings, A. R. Rahimi, and J. W. F. Goddard. : Microwave
441 links: The future for urban rainfall measurement, *Atmos. Res.*, 77, 300,
442 doi:10.1016/j.atmosres.2004.10.009, 2005.
- 443 Van het Schip, T. I., A. Overeem, H. Leijnse, R. Uijlenhoet, J. F. Meirink and A. J. van Delden:
444 Rainfall measurement using cell phone links: classification of wet and dry periods using
445 geostationary satellites, *Hydrological Sciences Journal*, DOI: 10.1080/02626667.2017.1329588,
446 2017.
- 447 Yilmaz, K. K., T. S. Hogue., K. S. Sorooshain., H. V. Gupta and T. Wagener.: Intercomparison of
448 Rain Gauge, Radar, and Satellite-Based Precipitation Estimates with Emphasis on Hydrologic
449 Forecasting, *American Meteorological Society*. Vol 6, 2005.
- 450 Zinevich, A., P. Alpert, and H. Messer.: Estimation of rainfall fields using commercial
451 microwave communication networks of variable density, *Adv. Water Resour.*, 31, 1470,
452 doi:10.1016/j.advwatres.2008.03.003, 2008.
- 453 Zinevich, A., H. Messer, and P. Alpert.: Frontal rainfall observation by a commercial microwave
454 communication network, *J. Appl. Meteorol. Climatol.*, 48, 1317, doi:10.1175/2008JAMC2014.1,
455 2009.
- 456 Zinevich, A., H. Messer, and P. Alpert.: Prediction of rainfall intensity measurement errors using
457 commercial microwave communication links, *Atmos. Measure. Tech.*, 3, 1385, doi:10.5194/amt-
458 3-1385-2010, 2010.